ChemComm RSCPublishing

COMMUNICATION

A General Method for the Fabrication of Graphene-Nanoparticle Hybrid Material

Cite this: DOI: 10.1039/x0xx00000x

Received 00th January 2012,
Accepted 00th January 2012

DOI: 10.1039/x0xx00000x

www.rsc.org/

Jaehyeung Park,[a] H. Surangi N. Jayawardena,[a] Xuan Chen,[a] Kalana W. Jayawardana,[a] Madanodaya Sundhoro,[a] Earl Ada,[b] and Mingdi Yan[a,*]

We describe a simple and general approach to conjugate nanoparticles on pristine graphene. The method takes advantage of the high reactivity of perfluorophenyl nitrene towards the C=C bonds in graphene, where perfluorophenyl azide-functionalized nanoparticles are conjugated to pristine graphene through the [2+1] cycloaddition reaction by a fast photoactivation.

Graphene-based hybrid nanomaterials have attracted much attention since the isolation of free-standing graphene becomes a reality. The unique and superior properties of graphene, such as high carrier mobility, high electrical and thermal conductivity as well as stability, make it an excellent candidate for the fabrication of novel hybrid nanomaterials. The hybrid nanomaterials can offer synergetic enhancement of material properties that may not be possible from each individual component. Various types of hybrid nanomaterials, especially those with nanoparticles, have been developed for a broad range of applications including catalysis,[1-3] sensor devices,[4, 5] fuel cells,[6, 7] solar cells,[8, 9] and therapeutics.[10] Most graphene-based hybrid nanomaterials used graphene oxide (GO) which is relatively easy to prepare in large quantities. Unlike pristine graphene, GO contains various oxygen-containing functional groups (carbonyl, carboxylic acid, epoxy, and hydroxyl) which can be used as reaction sites to covalently attach nanoparticles.[11-18] Several reactions have been employed for immobilizing nanoparticles including amidation,[11, 12] hydrolysis,[13] reduction,[14-17] and solvothermal process.[18] For example, Chan et al. conjugated iron oxide magnetic nanoparticles (MNPs) to GO by activating the carboxy group on GO with N-hydroxysuccinimide followed by coupling with amine-functionalized iron oxide MNPs.[11] The density of MNPs on GO could be varied by the concentration of MNPs in the feed. Another approach involves the in situ reduction of the nanoparticle precursor as well as GO to produce reduced GO-nanoparticle conjugates. For example, Kamat et al., employed ultrasonication of poly(ethylene glycol) to generate radicals which reduced both Au(III) and GO to produce gold nanoparticles on reduced graphene surface.[14]

The advantage of GO is the possibility of obtaining single-layer materials in large quantities. However, because GO is made by treating graphite with strong oxidation reagents, a subsequent reduction step, either chemical or thermal, is necessary to regain the property of graphene. Even after extensive reduction, oxygen species still remain. In addition, the harsh oxidation process could cleave the hexagonal framework causing permanent structural damage that cannot be restored. For example, Gómez-Navarro et al. reported that the conductivity and carrier mobility of reduced GO at room temperature decreased by 3 and 2 orders of magnitude, respectively.[19] In the case of in situ reduction of metal salts,[15-18] the morphology of the nanoparticles generated was difficult to control.[20]

In this article, we report a new method to synthesize graphene-nanoparticle conjugates using pristine graphene and pre-made nanoparticles. By using pristine graphene, no oxygen species are introduced and the materials are not subjected to harsh oxidation or reduction treatment. In addition, the nanoparticles are prepared in advance, and the size, shape and properties can be well controlled. To make the graphene-nanoparticle hybrid materials, the nanoparticles were functionalized with perfluorophenyl azide (PFPA), and the resulting nanoparticles were covalently attached to pristine graphene using the photocoupling chemistry developed in our laboratory.[21] Upon light activation, PFPA is converted to the singlet perfluorophenyl nitrene which subsequently reacts with C=C in graphene through [1+2] cycloaddition reaction.[22-26] Irradiation of the PFPA- functionalized nanoparticles in the presence of pristine

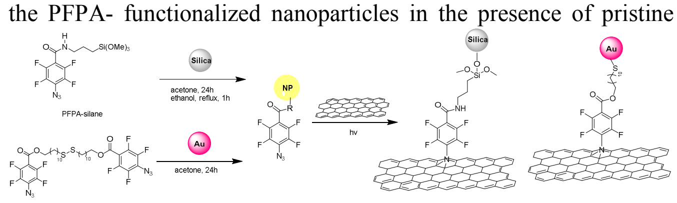

Scheme 1. Synthesis of graphene-nanoparticle conjugates.

graphene resulted in the conjugation of the nanoparticles on graphene. Three different types of pristine graphene were used based on the preparation method, including solvent-exfoliated few-layer graphene (FLG), and graphene prepared by micro-mechanical exfoliation and chemical vapor deposition (CVD)

To make liquid-exfoliated FLG, graphite flakes (50 mg, Sigma) were added to 1,2-dichlorobenzene (DCB) (20 mL), and the mixture was sonicated using a sonication probe (SONICS, 20 kHz, 40% Ampl.) for 30 min and then settled for 1 week. The supernatant was centrifuged at 4500 rpm for 30 min, and the upper solution was collected.[23] The concentration of FLG was determined to be 0.3 mg/mL by weighing the powder after drying the sample under vacuum. Mechanically exfoliated graphene was prepared using the scotch tape method.[27] Commercially available ZYH grade HOPG (highly oriented pyrolytic graphite, 5 mm x 5 mm x 1 mm, Union Carbide, USA) was peeled repeatedly for 15 times using a scotch tape, and was deposited by pressing the sample on a silicon wafer having an oxide layer of □300 nm thick. The wafer was then baked at 140 ^{o}C for 40 min. CVD graphene prepared on copper film was a gift from AIXTRON SE (Germany). The graphene samples prepared by the three methods were characterized by Raman spectroscopy (Bruker Senterra Raman microscope) at 532 nm excitation (Figure S1). The two peaks indicative of single-layer graphene were observed in the Raman spectra of mechanically exfoliated graphene and CVD graphene: the G band at ~1580 cm^{-1} which is due to the vibration mode of sp^2 carbon and the symmetric 2D band at ~2685 cm^{-1} which is from the second order vibration. Liquid exfoliated FLG flakes had a broad and asymmetric 2D band peak which is consistent with multilayer graphene, and the D band at 1370 cm^{-1} which is due to the defects resulting from the edge of graphene sheets.

Silica nanoparticles (SNPs) and gold nanoparticles (AuNPs) were used to demonstrate the method. PFPA-functionalized nanoparticles were prepared by treating SNPs and AuNPs with PFPA-silane[28] and PFPA-disulfide,[29] respectively, following the protocols developed previously in our laboratory (Scheme 1, see Supporting Information for experimental details). Figure 1 shows the TEM images and IR spectra of PFPA-functionalized nanoparticles. The average particle sizes were 81.2 ± 7.3 nm (Figure 1a) and 14.9 ± 1.5 nm (Figure 1b) for PFPA-SNP and PFPA-AuNP, respectively, measured by TEM. The asymmetric stretch of the azido group at 2126 cm^{-1}, the amide stretches at 1653 cm^{-1} for PFPA-SNP and the ester stretch at 1750 cm^{-1} for PFPA-AuNP were observed in the IR spectra (Figure 1c), indicating that the nanoparticles have been successfully functionalized by PFPA. To covalently conjugate nanoparticles on graphene, the graphene samples were treated with PFPA-functionalized nanoparticles by photoactivation (Scheme 1). For FLG, a dispersion of PFPA-functionalized SNPs or AuNPs in acetone was mixed with FLG flakes in *o*-dichlorobenzene and the mixture was irradiated with a medium-pressure Hg lamp for 30 min. Excess nanoparticles were removed by repetitive washing and centrifugation in acetone to afford nanoparticle-conjugated FLG. For mechanically exfoliated graphene or CVD graphene, the samples were immersed in a suspension of PFPA-SNPs or PFPA-AuNPs and were irradiated with medium pressure Hg lamp for 30 min. Figure 2 shows the images of SNPs and AuNPs covalently attached to FLG (a, d), mechanically exfoliated graphene (b, e), and CVD graphene (c, f). In all cases, nanoparticles distributed fairly evenly and were clearly attached on graphene without obvious distortion. Note that there were areas on CVD graphene samples that did not have nanoparticles (darker areas in Figure 2c, 2f). This is due to the defects in the CVD graphene starting material, i.e., areas on the wafer that did not have any deposited CVD graphene as shown in the Raman map of the CVD graphene (Figure S2).

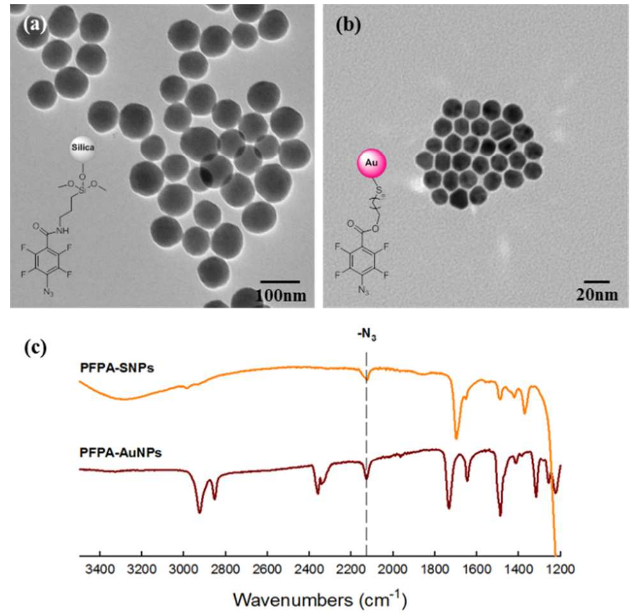

Fig. 1 TEM images of PFPA-functionalized nanoparticles: a) PFPA-SNPs and b) PFPA-AuNPs. c) IR spectra of corresponding samples.

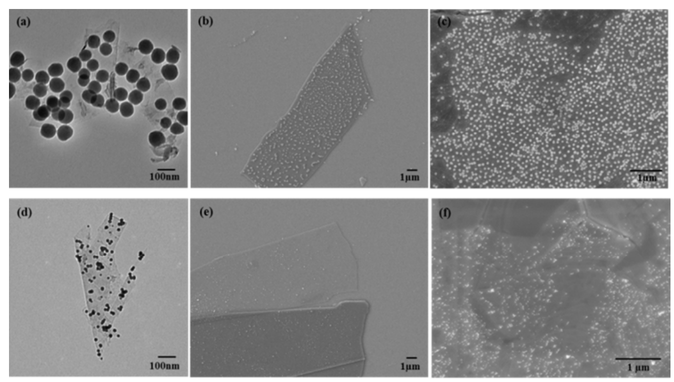

Fig. 2 Electron microscopy images of SNPs conjugated on a) FLG flakes, b) mechanically exfoliated graphene, (c) CVD graphene; and AuNPs conjugated on d) FLG flakes, e) mechanically exfoliated graphene, (f) CVD graphene.

To confirm that the nanoparticles were indeed covalently attached to graphene, control experiments were carried out where the graphene samples were treated with PFPA-functionalized nanoparticles under the same conditions except that no UV irradiation was applied. In this case, almost no particles were present on the graphene samples (Figure S3, S4), indicating that UV activation of PFPA was responsible for the covalent bond formation between nanoparticles and graphene. Additionally, when unfunctionalized nanoparticles were treated with graphene under the same conditions, very little nanoparticles were observed on graphene. This is in contrast with the many nanoparticles seen on covalently conjugated samples. The residual nanoparticles seen on the control samples (Figure S3, S4) are likely due to the non-specific physical adsorption of nanoparticles on graphene. These results demonstrated that the nanoparticles observed on graphene in Figure 2 are the results of the covalent bond formation between the PFPA-functionalized nanoparticles and graphene.

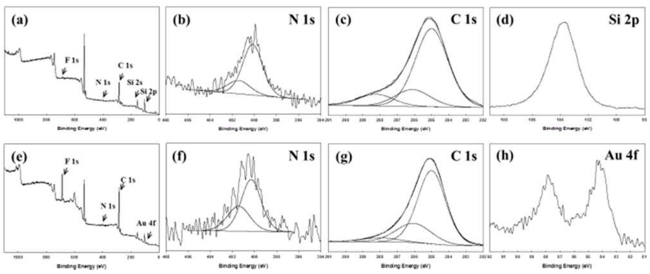

Fig. 3 XPS spectra of FLG conjugated with SNPs (a-d) and AuNPs (e-h).

X-ray photoelectron spectroscopy (XPS) was performed to further study the covalent bond formation between the nanoparticles and graphene. Figure 3 shows the survey and high resolution spectra of FLG flakes conjugated with SNPs (SNP-FLG, a-d) and AuNPs (AuNP-FLG, e-h). The XPS system is a Vacuum Generators Escalab MK II x-ray photoelectron spectrometer equipped with a dual Mg/Al x-ray source and with a 150 degree spherical sector electron energy analyzer operated in constant analyzer energy mode. The vacuum level during XPS analysis was at 1 x 10^{-9} torr. Survey and core level spectra were collected at pass energy of 100 eV and 50 eV, respectively. All spectra were referenced to the C1s binding energy position of adventitious carbon taken at 285.0 eV. The XPS spectra showed the anticipated F 1s and N 1s peaks, as well as the Si 2p peak in the SNP-FLG sample (Figure 3a, 3d) and the Au 4f peak in the AuNP-FLG sample (Figure 3e, 3h). The XPS of PFPA-functionalized surfaces has two N 1s peaks at 402.1 eV and 405.6 eV with the intensity ratio of 2:1, corresponding to the two outer and the one inner N of the azide.[30] After PFPA-functionalized NPs were conjugated to FLG, the XPS spectra of SNP-FLG (Figure 3b) and AuNP-FLG (Figure 3f) showed two N 1 s at 400.2 eV and 401.4 eV, repectively. The disappearance of the peak at 406.5 eV was a result from the loss of nitrogen when the azide decomposed upon photolysis. When PFPA-SNPs or PFPA-AuNPs were irradiated in the presence of FLG, only those PFPAs that were in contact with FLG would be involved in the covalent bond formation with FLG. The majority of PFPA on the nanoparticles, upon UV irradiation, gave singlet perfluorophenyl nitrene that could either react with the solvent DCB to give CH insertion products (i.e., aniline derivatives) or undergo intersystem crossing to triplet nitrene which then yields an aniline product.[31] Based on this, we assign the larger peak at 400.2 eV to the N in the various aniline products.[32] The N of the amide bond in PFPA-silane (Scheme 1) also shows up in the same region, thus contributing to the larger peak in Figure 3b.[33] The smaller peak at 401.4 eV was assigned to the N in the covalent structure formed between graphene and PFPA.[34, 35] The peaks at 285.0, 286.4, and 288.1 eV in the C 1s spectra are consistent with previous results of PFPA-functionalized graphene, and are assigned to C-C, C-N, and C-F and O=C-N, respectively (Figure 3c, 3g).[24] Taken together, the XPS results demonstrated that the nanoparticles were covalently bound on FLG through PFPA-mediated photocoupling chemistry.

Conclusions

In summary, we have successfully developed a general method to conjugate nanoparticles to pristine graphene for the synthesis of graphene-nanoparticle hybrid nanomaterials. This method takes advantage of the high reactivity of perfluorophenyl nitrene towards C=C bonds in graphene whereby PFPA-functionalized nanoparticles can be readily conjugated to graphene by a simple photoactivation of PFPA. The method applies to pristine graphene prepared by solvent exfoliation, mechanical exfoliation and CVD. By using pre-prepared nanoparticles, the size, shape, and morphology of nanoparticles can be controlled in advance. The type of nanoparticles is not limited to SNPs and AuNPs in this study so long as they are functionalized with PFPA. We have prepared a variety of PFPA-functionalized nanoparticles including iron oxide (Fe3O4),[36] quantum dots,[37] titanium dioxide nanoparticles, silver nanoparticles, and polymer nanoparticles. The method developed here could be readily used to synthesize graphene hybrid nanomaterials with these nanoparticles. The new method should pave the way for the fabrication of high performance graphene-based hybrid nanomaterials that can be utilized in applications including catalysis, nanoelectronics, sensing devices, and therapeutics.

Acknowledgment

This work was supported by NSF (CHE-1112436) and a startup fund from the University of Massachusetts Lowell.

Notes and references

[a] Department of Chemistry, University of Massachusetts Lowell, Lowell, Massachusetts 01854, United States, Fax: +1-978-334-33013; Tel: +1-978-334-3647; E-mail: mingdi_yan@uml.edu

[b] Materials Characterization Laboratory, University of Massachusetts Lowell, Lowell, Massachusetts 01854, United States

† Electronic Supplementary Information (ESI) available: Experimental details on the synthesis of nanoparticles and graphene-nanoparticle gonjugates, Raman spectra of graphene samples, and electron microscopy images of control samples are presented in supporting information. See DOI: 10.1039/c000000x/

1. G. M. Scheuermann, L. Rumi, P. Steurer, W. Bannwarth and R. Mülhaupt, *J. Am. Chem. Soc.*, 2009, **131**, 8262-8270.
2. I. V. Lightcap, T. H. Kosel and P. V. Kamat, *Nano Lett.*, 2010, **10**, 577-583.
3. I. V. Lightcap and P. V. Kamat, *J. Am. Chem. Soc.*, 2012, **134**, 7109-7116.
4. Q. Chen, L. Zhang and G. Chen, *Anal. Chem.*, 2011, **84**, 171-178.
5. Y. Wang, R. Yuan, Y. Chai, Y. Yuan, L. Bai and Y. Liao, *Biosens. Bioelectron.*, 2011, **30**, 61-66.
6. C. Venkateswara Rao, C. R. Cabrera and Y. Ishikawa, *J. Phys. Chem. C*, 2011, **115**, 21963-21970.
7. S. Yu, Q. Liu, W. Yang, K. Han, Z. Wang and H. Zhu, *Electrochim. Acta*, 2013, **94**, 245-251.
8. Y.-B. Tang, C.-S. Lee, J. Xu, Z.-T. Liu, Z.-H. Chen, Z. He, Y.-L. Cao, G. Yuan, H. Song, L. Chen, L. Luo, H.-M. Cheng, W.-J. Zhang, I. Bello and S.-T. Lee, *ACS Nano*, 2010, **4**, 3482-3488.
9. N. Yang, J. Zhai, D. Wang, Y. Chen and L. Jiang, *ACS Nano*, 2010, **4**, 887-894.
10. M.-C. Wu, A. R. Deokar, J.-H. Liao, P.-Y. Shih and Y.-C. Ling, *ACS Nano*, 2013, **7**, 1281-1290.
11. F. He, J. Fan, D. Ma, L. Zhang, C. Leung and H. L. Chan, *Carbon*, 2010, **48**, 3139-3144.
12. Y. Zhang, B. Chen, L. Zhang, J. Huang, F. Chen, Z. Yang, J. Yao and Z. Zhang, *Nanoscale*, 2011, **3**, 1446-1450.
13. Q. Qu, S. Yang and X. Feng, *Adv. Mater.*, 2011, **23**, 5574-5580.

14. K. Vinodgopal, B. Neppolian, I. V. Lightcap, F. Grieser, M. Ashokkumar and P. V. Kamat, *J. Phys. Chem. Lett.*, 2010, **1**, 1987-1993.
15. C. Xu, X. Wang and J. Zhu, *J. Phys. Chem. C*, 2008, **112**, 19841-19845.
16. G. Goncalves, P. A. A. P. Marques, C. M. Granadeiro, H. I. S. Nogueira, M. K. Singh and J. Grácio, *Chem. Mater.*, 2009, **21**, 4796-4802.
17. M. Zhang, B. Qu, D. Lei, Y. Chen, X. Yu, L. Chen, Q. Li, Y. Wang and T. Wang, *J. Mater. Chem.*, 2012, **22**, 3868-3874.
18. N. Li, Z. Geng, M. Cao, L. Ren, X. Zhao, B. Liu, Y. Tian and C. Hu, *Carbon*, 2013, **54**, 124-132.
19. C. Gómez-Navarro, R. T. Weitz, A. M. Bittner, M. Scolari, A. Mews, M. Burghard and K. Kern, *Nano Lett.*, 2007, **7**, 3499-3503.
20. H. Ismaili, D. Geng, A. X. Sun, T. T. Kantzas and M. S. Workentin, *Langmuir*, 2011, **27**, 13261-13268.
21. L.-H. Liu and M. Yan, *Acc. Chem. Res.*, 2010, **43**, 1434-1443.
22. L.-H. Liu and M. Yan, *Nano Lett.*, 2009, **9**, 3375-3378.
23. L.-H. Liu, M. M. Lerner and M. Yan, *Nano Lett.*, 2010, **10**, 3754-3756.
24. L.-H. Liu, G. Zorn, D. G. Castner, R. Solanki, M. M. Lerner and M. Yan, *J. Mater. Chem.*, 2010, **20**, 5041-5046.
25. L.-H. Liu and M. Yan, *J. Mater. Chem.*, 2011, **21**, 3273-3276.
26. J. Park and M. Yan, *Acc. Chem. Res.*, 2012, **46**, 181-189.
27. K. S. Novoselov, A. K. Geim, S. V. Morozov, D. Jiang, Y. Zhang, S. V. Dubonos, I. V. Grigorieva and A. A. Firsov, *Science*, 2004, **306**, 666-669.
28. J. P. Gann and M. Yan, *Langmuir*, 2008, **24**, 5319-5323.
29. X. Wang, O. Ramstroem and M. Yan, *J. Mater. Chem.*, 2009, **19**, 8944-8949.
30. G. Zorn, L.-H. Liu, L. Árnadóttir, H. Wang, L. J. Gamble, D. G. Castner and M. Yan, *J. Phys. Chem. C*, 2013, **118**, 376-383.
31. J. F. W. Keana and S. X. Cai, *J. Org. Chem.*, 1990, **55**, 3640-3647.
32. G. Beamson and D. Briggs, *J. Chem. Educ.*, 1993, **70**, A25.
33. S. A. Al-Bataineh, R. Luginbuehl, M. Textor and M. Yan, *Langmuir*, 2009, **25**, 7432-7437.
34. J. M. Minoo, Y. Wenrong, B. Barbara, R. G. Thomas, G. Mei, Z. Hadi and J. M. Maxine, *Nanotechnology*, 2012, **23**, 425503.
35. M. Dionisio, J. M. Schnorr, V. K. Michaelis, R. G. Griffin, T. M. Swager and E. Dalcanale, *J. Am. Chem. Soc.*, 2012, **134**, 6540-6543.
36. L.-H. Liu, H. Dietsch, P. Schurtenberger and M. Yan, *Bioconjugate Chem.*, 2009, **20**, 1349-1355.
37. H. S. N. Jayawardena, K. W. Jayawardana, X. Chen and M. Yan, *Chem. Commun.*, 2013, **49**, 3034-3036.